



## Synthesis, characterization, physical properties, and applications of highly fluorescent pyrene-functionalized 9,9-bis(4-diarylamino-phenyl)fluorene in organic light-emitting diodes

Narid Prachumrak, A-monrat Thangthong, Ruangchai Tarsang, Tinnagon Keawin, Siriporn Jungsuttiwong, Taweesak Sudyoasuk, Vinich Promarak\*

Center for Organic Electronic and Alternative Energy, Department of Chemistry and Center for Innovation in Chemistry, Faculty of Science, Ubon Ratchathani University, Warinchumrap, Ubon Ratchathani, 34190, Thailand

### ARTICLE INFO

#### Article history:

Received 11 May 2012

Revised 13 July 2012

Accepted 27 July 2012

Available online 2 August 2012

#### Keywords:

Pyrene

Fluorene

Blue-emitting material

Hole-transporting material

Organic light-emitting diode

### ABSTRACT

A new, highly fluorescent pyrene-functionalized 9,9-bis(4-diarylamino-phenyl)fluorene, namely **PTF**, was synthesized and characterized. This material is an amorphous molecular glass with notably high  $T_g$ , is electrochemically stable, and exhibits strong blue emission both in solution and solid state. It shows promising ability as a solution processed blue emitter and hole-transporter for OLEDs. High-efficiency sky-blue and Alq3-based green devices with luminance efficiencies of 1.13 and 4.08 cd/A are achieved, respectively.

© 2012 Elsevier Ltd. All rights reserved.

Organic light-emitting diodes (OLEDs) have attracted significant attention due to their applications as next-generation flat-screen displays and in general illumination.<sup>1</sup> In the past decade, we have seen great progress in both material development and device fabrication techniques.<sup>2</sup> One area of on-going research is the pursuit of a stable blue-emitting material.<sup>3</sup> Although, many types of blue light-emitting materials have been investigated, such as derivatives of anthracene, fluorene, and polycyclic aromatic hydrocarbons,<sup>3c,4</sup> further improvement for blue OLEDs compared to red and green devices is still required. Pyrene has also been widely used as a building block to form many emissive materials<sup>5</sup> due to its high photoluminescence efficiency in the blue spectrum, high carrier mobility, and improved hole-injection ability compared with other blue chromophores.<sup>6</sup> Though many pyrene-functionalized materials were proven to be promising blue emitters for OLEDs,<sup>7</sup> solution-processed analogues remain rare and largely unexplored in OLEDs.<sup>8</sup> To enhance the color purity of pyrene-based materials, it is essential to integrate either large bulky groups<sup>9</sup> or multi-substituted rigid moieties<sup>10</sup> to suppress aggregates and excimers. 9,9-Bis(4-diphenylamino-phenyl)fluorene possesses a highly rigid framework and has been successfully used as a building block to form many

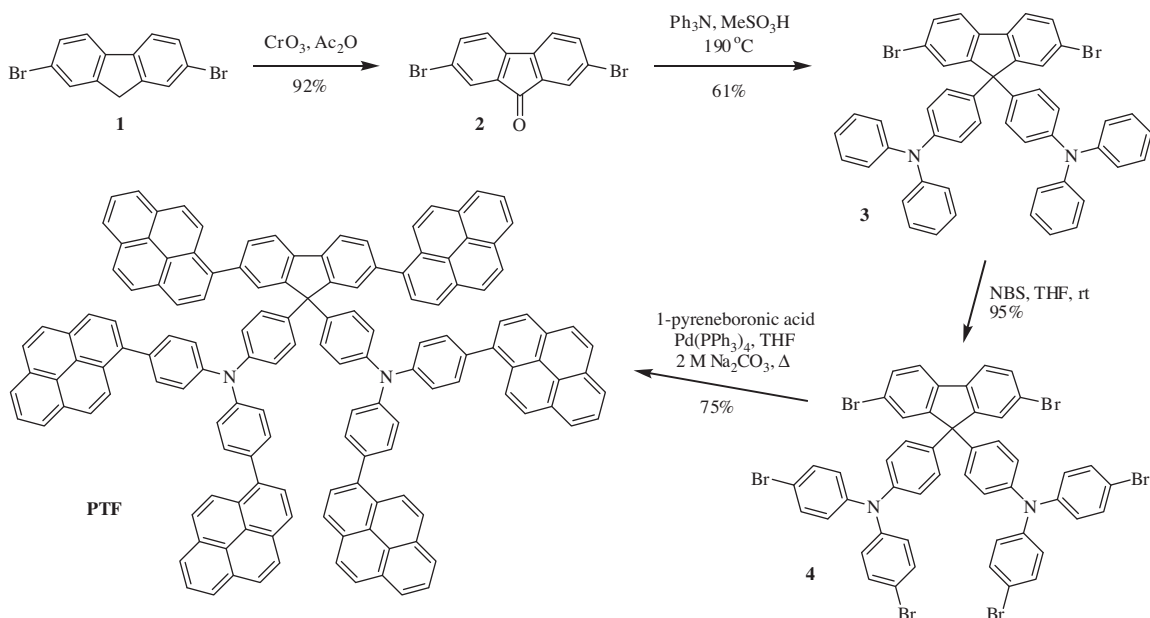
blue-emitting molecules and polymers with improved hole-injection, thermal stability, and suppressed aggregation.<sup>11</sup>

Therefore, we herein implemented all the required features in the synthesized molecule (Scheme 1). Incorporation of pyrene units into a cruciform of 9,9-bis(4-diphenylamino-phenyl)fluorene would offer an effective way to control the  $\pi$ - $\pi$  stacking interactions and the associated red shift in emission, and maintain the high blue emissive ability of pyrene in the solid state. Moreover, triarylamino units also improve hole injection and transport ability with high thermal stability. Owing to its supramolecular steric hindrance, the material would possess good solubility and hence a thermally stable amorphous thin film could be deposited by a cheap solution process. Accordingly, this would result in a new solution-processable molecular material with combined blue-emitting and hole-transporting properties for OLEDs.

In this work, we present the synthesis and characterization of such a material, namely 9,9-bis{4-di[4-(pyren-2-yl)phenyl]amino-phenyl}-2,7-di(pyren-2-yl)fluorene (**PTF**). An investigation of its physical and photophysical properties, and its application as active layers in OLEDs are also reported. Scheme 1 outlines the synthesis of the designed molecule, **PTF**. We began with the aerial oxidation of 2,7-dibromofluorene (**1**) with KOH/air in DMSO to give 2,7-dibromofluorenone (**2**) as a yellow solid in a low yield of 31% and 2-bromofluorenone was also isolated in 23% as a by-product. An improved 92% yield of fluorenone **2** was obtained by oxidation of **1**

\* Corresponding author.

E-mail addresses: [pvnich@ubu.ac.th](mailto:pvnich@ubu.ac.th), [pvnich@gmail.com](mailto:pvnich@gmail.com) (V. Promarak).

Scheme 1. Synthesis of **PTF**.

with  $\text{CrO}_3$  in acetic anhydride along with a trace amount of 2-bromofluorenone. The 9,9-bis(4-diphenylaminophenyl)fluorene (**3**) intermediate was then synthesized via a tandem protocol involving the reaction of fluorenone **2** with excess triphenylamine catalyzed by  $\text{MeSO}_3\text{H}$  at  $190^\circ\text{C}$ . Product **3** was obtained as a white solid in 61% yield. Selective bromination of compound **3** with NBS in THF gave 9,9-bis[4-di(4-bromophenyl)aminophenyl]-2,7-dibromofluorene (**4**) as a white solid in excellent yield. Coupling of the resultant hexabromide **4** with readily available 1-pyrene boronic acid under Suzuki cross-coupling conditions catalyzed by  $\text{Pd}(\text{PPh}_3)_4/\text{Na}_2\text{CO}_3$  (aq) in THF afforded **PTF** as a light-yellow solid in a good yield of 75%. The structure was characterized unambiguously by NMR spectroscopy and mass spectrometry.<sup>12</sup> **PTF** showed good solubility in organic solvents, opening the door to solution processing techniques.

Quantum chemical calculations on **PTF** performed using the TDDFT/B3LYP/6-31G(d,p) method<sup>13</sup> revealed that the two triarylamine units at the C-9 position of the fluorene ring generated high steric hindrance, resulting in a bulky molecular structure with high steric repulsion between the aromatic rings and thereby preventing close  $\pi$ - $\pi$  stacking interactions and imparting good ability to dissolve in a solvent (Supplementary data). In the HOMO, electrons are delocalized over the pyrene-triphenylamine moiety resulting in less  $\pi$ -electron interactions between the fluorene and pyrene moieties, while in the LUMO, the excited electrons are delocalized over the quinoid-like pyrene-fluorene plane. The HOMO-LUMO energy gap ( $E_g$  calcd) was calculated to be 3.01 eV which slightly deviated from that estimated from the optical absorption edge (2.97 eV). There are factors responsible for errors in the  $E_g$  calcd values because the orbital energy difference between the HOMO and LUMO is still an approximate estimation of the transition energy which also contains significant contributions from some two-electron integrals. The real situation is that an accurate description of the lowest singlet excited state requires a linear combination of a number of excited configurations.

In a  $\text{CH}_2\text{Cl}_2$  solution, the absorption spectrum of **PTF** showed bands at 279 and 364 nm, while the photoluminescence spectrum displayed a featureless emission peak at 478 nm (Fig. 1). In the solid state, the emission spectrum of the thin film obtained by spin-coating on a quartz substrate was identical to its solution spectrum. This suggested that the bulky molecular structure of **PTF** reduced

effectively the intermolecular  $\pi$ - $\pi$  interactions of the pyrene units in the solid state. This material exhibited strong blue fluorescence in both solution and solid state with a high solution fluorescence quantum yield ( $\Phi_F$ ) of 0.85. A cyclic voltammetry (CV) study on **PTF** revealed a quasi-reversible oxidation wave at 0.86 V with no distinct reduction process being detected (Fig. 2a). The oxidation assigned to removal of electrons from the triphenylamine-pyrene resulting radical cations occurred at a lower potential value than that of other triarylamine derivatives having *p*-unsubstituted phenyl rings ( $E_{1/2} = 0.93$  V),<sup>14</sup> supporting the existence of  $\pi$ -electron interactions between the triphenylamine and substituted pyrene as revealed by the calculations. Multiple CV scans displayed identical CV curves indicating an electrochemically stable molecule. The HOMO and LUMO levels of **PTF** were calculated to be 5.21 and 2.24 eV, respectively.

Thermogravimetric analysis (TGA) revealed that **PTF** was thermally stable with a 5% weight loss ( $T_{5d}$ ) at a temperature well over  $475^\circ\text{C}$  (Fig. 2b). In repeated differential scanning calorimetry (DSC), all the thermograms displayed only endothermic baseline shifts owing to glass transition ( $T_g$ ) at  $237^\circ\text{C}$  with no crystallization and melting being observed at higher temperatures, indicating a highly stable amorphous material. The  $T_g$  value of this material is among the highest values in amorphous hole-transporting materials (AHTMs) reported so far, and is significantly higher than those of the most widely used HTMs, *N,N*-diphenyl-*N,N'*-bis(1-naphthyl)-(1,1'-biphenyl)-4,4'-diamine (NPB) ( $T_g = 100^\circ\text{C}$ ) and *N,N'*-bis(3-methylphenyl)-*N,N'*-bis(phenyl)benzidine (TPD) ( $T_g = 63^\circ\text{C}$ ).<sup>15</sup> The amorphous features of **PTF** were further studied by powder X-ray diffraction (XRD) using silicon wafer as a substrate. Its XRD pattern showed broad diffraction peaks between  $10.5$  and  $34.6^\circ$  with characteristic peaks ascribed to the  $\pi$ - $\pi$  stacking of pyrene units being observed (Supplementary data). The morphology of **PTF** was characterized by atomic force microscopy. The film spin-coated from THF:toluene solution showed quite a smooth surface indicating its good film-forming ability (Supplementary data). These results proved that the use of 9,9-bis(4-diarylaminophenyl)fluorene as a molecular platform could reduce the crystallization of pyrene and improve the amorphous stability of the material, which in turn could increase the service time in device operation and enhance the morphological stability of the thin film. Moreover, the ability

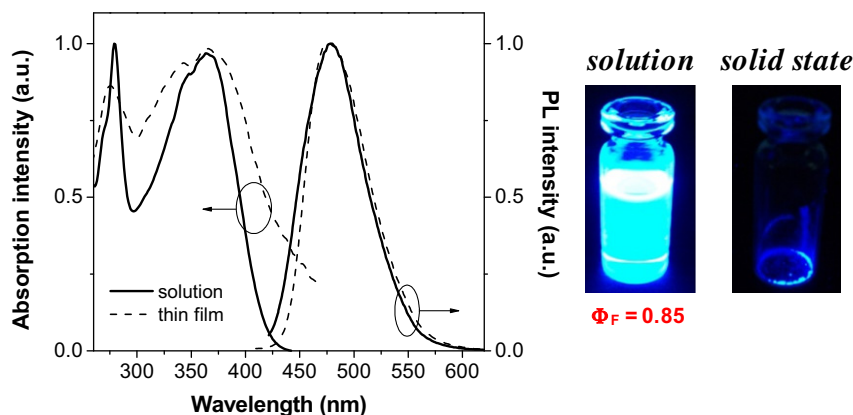


Figure 1. UV-Vis absorption and PL spectra in solution ( $\text{CH}_2\text{Cl}_2$ ) and as a thin film.

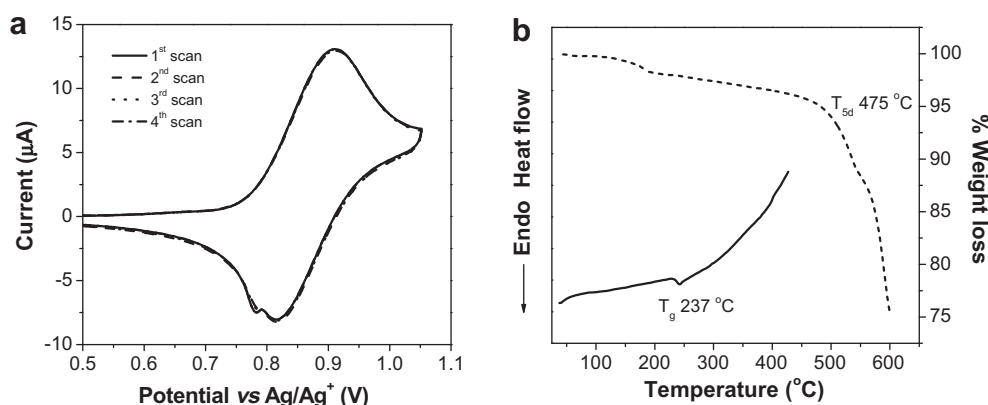


Figure 2. (a) Multiple CV curves measured in  $\text{CH}_2\text{Cl}_2$  at a scan rate of 50 mV/s. (b) DSC (2<sup>nd</sup> scan), and TGA curves measured at 10 °C/min under  $\text{N}_2$ .

of **PTF** to form a good thin film by solution casting techniques is highly desirable for fabrication of cheap OLED devices.

The properties of **PTF** as a blue emissive layer (EML) and hole-transporting layer (HTL) in OLEDs were investigated. Devices with structures: ITO/PEDOT:PSS/EML (40 nm)/BCP (40 nm)/LiF (0.5 nm):Al (150 nm) and ITO/PEDOT:PSS/HTL (40 nm)/Alq3 (50 nm)/LiF (0.5 nm):Al (150 nm) were fabricated. The **PTF** layer in both devices was spin-coated from THF:toluene (1:1) solution with controlled thickness. To compare the bifunctional ability of **PTF**, commercially available NPB was employed as a reference EML and HTL material, and the reference devices **II**, **IV**, and **V** were fabricated using the same structure and device fabrication processes. The electroluminescent (EL) spectra and current density-voltage-luminance ( $I$ - $V$ - $L$ ) characteristics of the devices are shown in Figure 3, and their electrical parameters are summarized in Table 1. As a blue emitter, the **PTF**-based device **I** exhibited a high maximum brightness of 5997  $\text{cd m}^{-2}$  (blue OLED) at 10.2 V, a low turn-on voltage of 3.2 V, and a maximum luminance efficiency of 1.13  $\text{cd A}^{-1}$  (Fig. 3 and Table 1). The operating voltage at 100  $\text{cd m}^{-2}$  was 4.8 V indicating that good performance was achieved. The device characteristics in terms of maximum brightness, turn-on voltage, and maximum luminous efficiency clearly demonstrated that the solution-processed blue-emitting ability of **PTF** was greater than the NPB-based device **II**. Under applied voltage, device **I** emitted a bright sky-blue luminescence with peaks centered at 474 nm and  $CIE$  coordinates of  $x = 0.15$  and  $y = 0.24$ . The EL spectrum of the diode matched with the PL spectrum of **PTF**. No emission shoulder at a longer wavelength due to excimer and exciplex species formed at the interface of the EML and BCP

layers, which often occurs in devices fabricated from EMLs with planar molecular structure,<sup>16</sup> was detected. This shoulder emission (at 463 nm) was observed in the NPB-based blue OLED (device **II**). In our case, the formation of these species might be prevented by the bulky nature of 9,9-bis(4-diarylamino)fluorene used as the molecular platform of **PTF**. Moreover, stable emission was obtained from device **I** and the EL spectra did not change over the entire driven voltages.

As a HTL, the **PTF**-based device **III** exhibited good performance with a high maximum brightness of 19560  $\text{cd m}^{-2}$  as a green OLED at 10.8 V, a low turn-on voltage of 3.0 V, and a maximum luminance efficiency of 4.08  $\text{cd A}^{-1}$  (Fig. 3 and Table 1). The operating voltage at 100  $\text{cd m}^{-2}$  was 4.2 V indicating that good performance was achieved. By comparison with the reference device **V**, it was found that the incorporation of **PTF** as a HTL not only increased the maximum luminance from 4961  $\text{cd m}^{-2}$  ( $\eta$  of 0.91  $\text{cd A}^{-1}$ ) in device **V** to 19560  $\text{cd m}^{-2}$  ( $\eta$  of 4.08  $\text{cd A}^{-1}$ ) in device **III**, but also significantly decreased the turn-on voltage from 4.2 V to 3.0 V. Besides, their EL spectra were nearly identical. Moreover, the device characteristics in terms of luminous efficiency clearly verified that the solution-processed HTM ability of **PTF** was greater than that of the NPB-based device **IV**. Device **III** emitted a bright green luminescence with EL spectra matching with the PL spectrum of Alq3, and the EL of the reference devices and other reported devices.<sup>17</sup> No emission at a longer wavelength due to exciplex species formed at the interface of the HTL and ETL materials, which often occurs in the devices fabricated from HTLs with planar molecular structures, was detected.<sup>18</sup> More importantly, a stable emission was obtained from this diode with the EL spectra and  $CIE$  coordinates not chang-

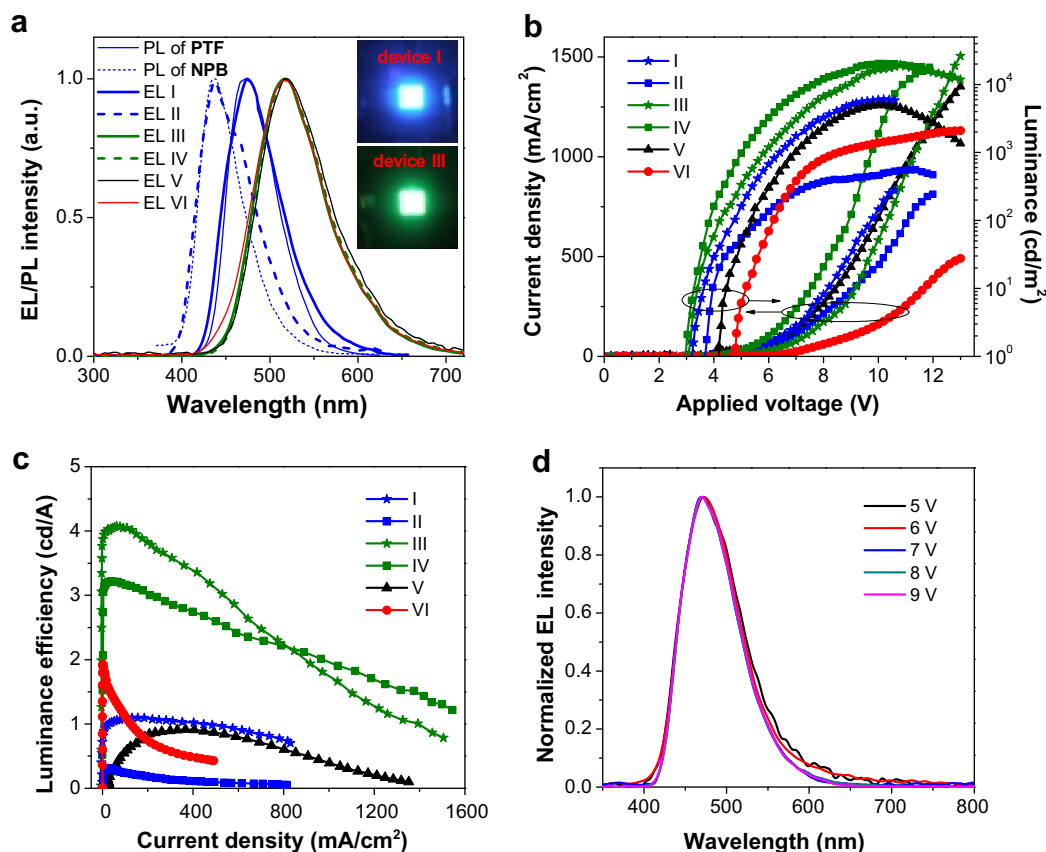


**Figure 3.** (a) EL spectra, (b) *I*-*V*-*L* characteristics, (c) variation of  $\eta$ -*I* of the fabricated OLEDs, and (d) normalized EL spectra of device **I** under different applied voltages.

**Table 1**

Device characteristics of OLEDs fabricated with **PTF** (**II** and **III**) and **NPB** (**II** and **IV**) as EMLs or HTLs

Device	Structure	Turn-on voltage (V) <sup>a</sup>	Emission maxima (nm)	Maximum luminance (L, cd m <sup>-2</sup> )	Luminance efficiency ( $\eta$ , cd A <sup>-1</sup> )	CIE coordinates (x, y)
<b>I</b>	ITO/PEDOT:PSS/ <b>PTF</b> /BCP/LiF:Al	3.2	474	5997	1.13	0.15, 0.24
<b>II</b>	ITO/PEDOT:PSS/ <b>NPB</b> /BCP/LiF:Al	3.7	438	558	0.31	0.16, 0.10
<b>III</b>	ITO/PEDOT:PSS/ <b>PTF</b> /Alq3/LiF:Al	3.0	518	19560	4.08	0.29, 0.53
<b>IV</b>	ITO/PEDOT:PSS/ <b>NPB</b> /Alq3/LiF:Al	3.0	518	20373	3.22	0.29, 0.53
<b>V</b>	ITO/PEDOT:PSS/Alq3/LiF:Al	4.2	518	4961	0.91	0.30, 0.54

<sup>a</sup> At a luminance of 1 cd m<sup>-2</sup>.

ing over the entire applied voltages (Supplementary data). Although, many blue emitting and hole-transporting materials have been reported, in terms of their amorphous morphology, significantly high  $T_g$  value solution processability and device efficiency, **PTF** is among the good bifunctional materials reported to date.

In summary, we have designed and synthesized **PTF** as a highly fluorescent blue light-emitting small molecule for OLEDs. Using 9,9-bis(4-diarylamino)fluorene as a molecular platform, we were able to reduce the crystallization and maintained the high blue emissive ability of pyrene in the solid state, and improved the amorphous stability of the material. **PTF** is an amorphous molecular glass with a very high  $T_g$ , is electrochemically stable, and exhibits strong blue emission both in solution and solid state. Its ability as both a blue light-emitter for blue OLEDs and hole-transporter for green OLEDs, in terms of device performance and thermal properties, was superior than commonly used **NPB**. Non-doped sky-blue and green OLEDs with luminance efficiencies of 1.13 and 4.08 cd/A were achieved, respectively.

## Acknowledgements

This work was supported financially by the Thailand Research Fund (RMU5080052), Center for Excellence in Innovation in Chemistry, Ubon Ratchathani University, and the Strategic Scholarships for Frontier Research Network for Research Groups (CHE-RES-RG50) from the Office of the Higher Education Council, Thailand. We acknowledge the scholarship support for N. Prachumrak from the Science Achievement Scholarship of Thailand (SAST).

## Supplementary data

Supplementary data associated with this article can be found, in the online version, at <http://dx.doi.org/10.1016/j.tetlet.2012.07.112>.

## References and notes

- (a) D'Andrade, B. W.; Forrest, S. R. *Adv. Mater.* **2004**, *16*, 1585–1585; (b) Grimsdale, A. C.; Chan, K. L.; Martin, R. E.; Jokisz, P. G.; Holmes, A. B. *Chem. Rev.* **2009**, *109*, 897–1091; (c) Lo, S. C.; Burn, P. L. *Chem. Rev.* **2007**, *107*, 1097–1116.

2. (a) Wu, C. H.; Chien, C. H.; Hsu, F. M.; Shih, P. I.; Shu, C. F. *J. Mater. Chem.* **2009**, *19*, 1464–1470; (b) Zhao, Z.; Deng, C.; Chen, S.; Lam, J. W. Y.; Qin, W.; Lu, P.; Wang, Z.; Kwok, H. S.; Ma, Y.; Qiu, H.; Tang, B. Z. *Chem. Commun.* **2011**, *47*, 8847–8849.
3. (a) Poriel, C.; Rault-Berthelot, J.; Thirion, D.; Barrière, F.; Vignau, L. *Chem. Eur. J.* **2011**, *17*, 14031–14046; (b) Xiao, L. X.; Su, S. J.; Agata, Y.; Lan, H. L.; Kido, J. *Adv. Mater.* **2009**, *21*, 1271–1274; c) Thangthong, A.; Meunmart, D.; Prachumrak, N.; Jungsuttiwong, S.; Keawin, T.; Sudyoadsuk, T.; Promarak, V. *Chem. Commun.* **2011**, *47*, 7122–7124.
4. Wu, Y.; Hao, X.; Wu, J.; Jin, J.; Ba, X. *Macromol.* **2010**, *43*, 731–738.
5. Figueira-Duarte, T. M.; Müllen, K. *Chem. Rev.* **2011**, *111*, 7260–7314.
6. Jia, W. L.; Cormick, T. M.; Liu, Q. D.; Fukutani, H.; Motala, M.; Wang, R. Y.; Tao, Y.; Wang, S. J. *J. Mater. Chem.* **2004**, *14*, 3344–3350.
7. (a) Tonzola, C. J.; Kulkarni, A. P.; Gifford, A. P.; Kaminsky, W.; Jenekhe, S. A. *Adv. Funct. Mater.* **2001**, *17*, 863–874; (b) Tang, C.; Liu, F.; Xia, Y. J.; Lin, J.; Xie, L. H.; Zhong, G. Y.; Fan, Q. L.; Huang, W. *Org. Electron.* **2006**, *7*, 155–162; c) Tang, C.; Liu, F.; Xia, Y. J.; Xie, L. H.; Wei, A.; Li, S. B.; Fan, Q. L.; Huang, W. *J. Mater. Chem.* **2006**, *16*, 4074–4080.
8. (a) Liu, F.; Tang, C.; Chen, Q. Q.; Shi, F. F.; Wu, H. B.; Xie, L. H.; Peng, B.; Wei, W.; Cao, Y.; Huang, W. *J. Phys. Chem. C* **2009**, *113*, 4641–4647; (b) Sonar, P.; Soh, M. S.; Cheng, Y. H.; Henssler, J. T.; Sellinger, A. *Org. Lett.* **2010**, *12*, 3292–3295.
9. Tao, S. L.; Zhou, Y. C.; Lee, C. S.; Zhang, X. H.; Lee, S. T. *Chem. Mater.* **2010**, *21*, 2138–2141.
10. Wang, Z. Q.; Xu, C.; Wang, W. Z.; Fu, W. J.; Niu, L. B.; Ji, B. M. *Solid-State Electron.* **2010**, *54*, 524–526.
11. (a) Ego, C.; Grimsdale, A. C.; Uckert, F.; Yu, G.; Srdanov, G.; Müllen, K. *Adv. Mater.* **2002**, *14*, 809–811; (b) Thangthong, A.; Prachumrak, N.; Tarsang, R.; Keawin, T.; Jungsuttiwong, S.; Sudyoadsuk, T.; Promarak, V. *J. Mater. Chem.* **2012**, *22*, 6869–6877; c) Surin, M.; Hennebicq, E.; Ego, C.; Marsitzky, D.; Grimsdale, A. C.; Müllen, K.; Brédas, J.-L.; Lazzaroni, R.; Leclère, P. *Chem. Mater.* **2004**, *16*, 994–1001; d) El-Khouly, M. E.; Chen, Y.; Zhuang, X.; Fukuzumi, S. *J. Am. Chem. Soc.* **2009**, *131*, 6370–6371; e) Fang, Q.; Xua, B.; Jiang, B.; Fua, H.; Zhuh, W.; Jiang, X.; Zhang, Z. *Synth. Met.* **2005**, *155*, 206–210; f) Tao, S.; Zhou, Y.; Lee, C.-S.; Zhang, X.; Lee, S.-T. *Chem. Mater.* **2010**, *22*, 2138–2141.
12. Characterization data for **3**: white solid;  $^1\text{H NMR}$  (300 MHz,  $\text{CDCl}_3$ )  $\delta$  6.99 (4H, d,  $J = 9.0$  Hz), 7.00 (8H, t,  $J = 9.0$  Hz), 7.09 (8H, d,  $J = 9.0$  Hz), 7.26 (8H, t,  $J = 9.0$  Hz), 7.55 (4H, t,  $J = 9.0$  Hz) and 7.58 (2H, d,  $J = 9.0$  Hz) ppm;  $^{13}\text{C NMR}$  (75 MHz,  $\text{CDCl}_3$ )  $\delta$  64.65, 121.55, 121.76, 122.77, 123.06, 124.5, 124.68, 128.69, 129.27, 129.38, 130.82, 137.66, 137.98, 146.74, 147.52 and 153.47 ppm; HRMS  $m/z$  calcd for  $\text{C}_{49}\text{H}_{34}\text{Br}_2\text{N}_2$ , 808.1089; found, 809.1169 [MH $^+$ ]. Compound **4**: white solid; mp. >250 °C;  $^1\text{H NMR}$  (300 MHz,  $\text{CDCl}_3$ )  $\delta$  6.93 (12H, t,  $J = 9.01$  Hz), 7.02 (4H, d,  $J = 8.40$  Hz), 7.36 (8H, d,  $J = 8.70$  Hz), 7.51 (4H, d,  $J = 6.90$  Hz) and 7.61 (2H, d,  $J = 8.40$  Hz) ppm;  $^{13}\text{C NMR}$  (75 MHz,  $\text{CDCl}_3$ )  $\delta$  115.95, 121.68, 121.85, 123.33, 125.92, 128.92, 129.28, 131.03, 132.43, 137.98 and 146.18 ppm; HRMS  $m/z$  calcd for  $\text{C}_{49}\text{H}_{30}\text{Br}_6\text{N}_2$ , 1126.1999; found, 1126.7604 [M $^+$ ]. Compound **PTF**: light-yellow solid; mp. >250 °C;  $^1\text{H NMR}$  (300 MHz,  $\text{CDCl}_3$ )  $\delta$  7.33 (5H, d,  $J = 8.40$  Hz), 7.42 (8H, d,  $J = 8.40$  Hz), 7.50–7.58 (11H, m), 7.71 (3H, t,  $J = 7.50$  Hz), 7.79 (3H, d,  $J = 7.50$  Hz), 7.97 (15H, t,  $J = 7.50$  Hz), 8.04–8.12 (20H, m), 8.17 (10H, t,  $J = 7.50$  Hz) and 8.24–8.30 (9H, m) ppm;  $^{13}\text{C NMR}$  (75 MHz,  $\text{CDCl}_3$ )  $\delta$  120.58, 123.96, 124.43, 124.69, 124.75, 124.87, 124.96, 125.01, 125.05, 125.14, 125.23, 125.35, 125.95, 127.30, 127.41, 127.56, 127.64, 128.46, 128.53, 128.94, 129.42, 130.20, 130.42, 130.67, 130.83, 131.00, 131.43, 131.51 and 131.54 ppm; HRMS  $m/z$  calcd for  $\text{C}_{145}\text{H}_{84}\text{N}_2$ , 1854.2319; found, 1853.5410 [M $^+$ ].
13. Frisch, M. J.; Trucks, G. W.; Schlegel, H. B.; Scuseria, G. E.; Robb, M. A.; Cheeseman, J. R.; Montgomery, J. A.; Jr.; Vreven, T.; Kudin, K. N.; Burant, J. C.; Millam, J. M.; Iyengar, S. S.; Tomasi, J.; Barone, V.; Mennucci, B.; Cossi, M.; Scalmani, G.; Rega, N.; Petersson, G. A.; Nakatsuji, H.; Hada, M.; Ehara, M.; Toyota, K.; Fukuda, R.; Hasegawa, J.; Ishida, M.; Nakajima, T.; Honda, Y.; Kitao, O.; Nakai, H.; Klene, M.; Li, X.; Knox, J. E.; Hratchian, H. P.; Cross, J. B.; Adamo, C.; Jaramillo, J.; Gomperts, R.; Stratmann, R. E.; Yazyev, O.; Austin, A. J.; Cammi, R.; Pomelli, C.; Ochterski, J. W.; Ayala, P. Y.; Morokuma, K.; Voth, G. A.; Salvador, P.; Dannenberg, J. J.; Zakrzewski, V. G.; Dapprich, S.; Daniels, A. D.; Strain, M. C.; Farkas, O.; Malick, D. K.; Rabuck, A. D.; Raghavachari, K.; Foresman, J. B.; Ortiz, J. V.; Cui, Q.; Baboul, A. G.; Clifford, S.; Cioslowski, J.; Stefanov, B. B.; Liu, G.; Liashenko, A.; Piskorz, P.; Komaromi, I.; Martin, R. L.; Fox, D. J.; Keith, T.; Al-Laham, M. A.; Peng, C. Y.; Nanayakkara, A.; Challacombe, M.; Gill, P. M. W.; Johnson, B.; Chen, W.; Wong, M. W.; Gonzalez, C.; Pople, J. A. *Gaussian 98*, revision A.7; Gaussian, Inc.: Pittsburgh, PA, **1998**.
14. Promarak, V.; Ichikawa, M.; Sudyoadsuk, T.; Saengsuwan, S.; Keawin, T. *Opt. Mater.* **2007**, *30*, 364–369.
15. Koene, B. E.; Loy, D. E.; Thompson, M. E. *Chem. Mater.* **1998**, *10*, 2235–2250.
16. Lai, K. Y.; Chu, T. M.; Hong, F. C. N.; Elangovan, A.; Kao, K. M.; Yang, S. W.; Ho, T. I. *Surf. Coat. Tech.* **2006**, *200*, 3283–3288.
17. (a) Kim, Y. K.; Hwang, S. H. *Synth. Met.* **2006**, *156*, 1028–1035; (b) Thangthong, A.; Saengsuwan, S.; Jungsuttiwong, S.; Keawin, T.; Sudyoadsuk, T.; Promarak, V. *Tetrahedron Lett.* **2011**, *52*, 4749–4752.
18. Kim, D. Y.; Cho, H. N.; Kim, C. Y. *Prog. Polym. Sci.* **2000**, *25*, 1089–1139.